A Unified Mathematical Approach to Two-Port Calibration Techniques and Some Applications

ROBERT A. SOARES, MEMBER, IEEE, PASCAL GOUZIEN, PIERRE LEGAUD, AND GEORGES FOLLOT

Abstract —**A rigorous mathematical treatment of microwave network analyzer calibration and de-embedding procedures for the two-port error network representation is employed in order to explain current calibration techniques in a succinct and homogeneous manner. It is demonstrated that the essence of through-delay de-embedding techniques consists in the use of two known two-port calibration standards to obtain pairs of similar matrices for the input and output error adapters. Once the characteristic vectors for these matrices are obtained, a number of different approaches may be employed in order to solve for the scaling constants.**

I. Introduction

Although the concepts underlying the through-delay-reflect de-embedding technique were first enunciated in 1975 [1], and numerous articles have subsequently appeared describing various aspects of this method [2]–[8], a unified and concise treatment of the problem has not, to the authors' knowledge, been presented.

The object of this paper is to present a simple mathematical formulation of this method so as to enable the basic concepts to be clearly grasped, thereby opening the way to innovative solutions to particular measurement problems. Two such problems are dealt with in this paper, by way of example: the case of a two-port network composed of symmetrical error adapters and the case of a device-under-test mounted in a non-50-Ω environment.

The traditional approach to error correction is via a flow-graph representation of the errors involved. However, if the flow graph permits an insight into the physical causes behind the transmission and reflection errors observed, it often obscures some simple and elegant mathematical solutions. A hybrid approach combining flow graphs and mathematics favored by some authors is, in our opinion, often confusing. For these reasons only the mathematical formulation is proposed in this paper.

II. Mathematical Formulation

A. Presentation of the Problem

Fig. 1 represents a typical two-port measurement problem: an unknown two-port network is to be measured via two unknown two-port error matrices X and Y [4]. As is typical in the two-port error adapter representation, errors due to leakage paths between error matrices X and Y and errors linked to the variation of source and load impedances with the measurement path are neglected. It is necessary to solve the error matrices X and Y by a "calibration" procedure before the unknown two-port can be measured. One method of doing this is to replace the unknown device-under-test with *two known transmission* devices, in general a back-to-back connection of X and Y (through) and a nonreflective 50 Ω line of known electrical length (delay).

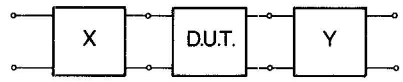

Fig. 1. Typical two-port measurement problem: extraction of device-under-test data from two-port measurement data including error adapters X and Y.

Manuscript received October 11, 1988; revised June 12, 1989.
The authors are with LAB/MER/MLS, Centre National d'Etudes des Telecommunications, B.P. 40, Lannion 22301 Cedex, France.
IEEE Log Number 8930520.

B. Calibration with Transmission Lines

The use of the through and delay line connection procedure, in its most general form, is summarized in Fig. 2. It can be mathematically represented using R or cascade matrices as follows [4], [9]:

$$\boldsymbol{R}_{M1} = \boldsymbol{R}_X \cdot \boldsymbol{R}_{T1} \cdot \boldsymbol{R}_Y \tag{1}$$

$$\boldsymbol{R}_{M2} = \boldsymbol{R}_X \cdot \boldsymbol{R}_{T2} \cdot \boldsymbol{R}_Y \tag{2}$$

where $\boldsymbol{R}_{M1}$ refers to the R-matrix equivalent of the S parameters measured via a two-port connecting R matrix $\boldsymbol{R}_{T1}$, and $\boldsymbol{R}_{M2}$ refers to the R-matrix equivalent of the S parameters measured via a two-port connecting R matrix $\boldsymbol{R}_{T2}$.

A solution in terms of the error network X is obtained by substituting for $\boldsymbol{R}_Y$ in (1) and (2) [9]:

$$\boldsymbol{R}_M \cdot \boldsymbol{R}_X = \boldsymbol{R}_X \cdot \boldsymbol{R}_T \tag{3}$$

with

$$\boldsymbol{R}_M = \boldsymbol{R}_{M2} \cdot (\boldsymbol{R}_{M1})^{-1} = \begin{bmatrix} m_{11} & m_{12} \\ m_{21} & m_{22} \end{bmatrix} \tag{4}$$

and

$$\boldsymbol{R}_T = \boldsymbol{R}_{T2} \cdot (\boldsymbol{R}_{T1})^{-1}. \tag{5}$$

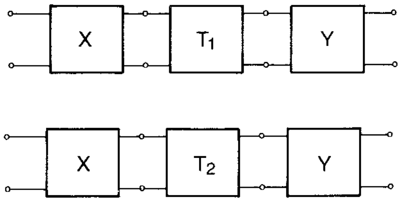

Fig. 2. Use of two known two-port networks T_1 and T_2 to solve for error adapters $\boldsymbol{X}$ and $\boldsymbol{Y}$.

The error matrix $\boldsymbol{Y}$ may be addressed in an identical manner by substituting for $\boldsymbol{R}_X$ in (1) and (2) [9]. Thus

$$\boldsymbol{R}_Y \cdot \boldsymbol{R}_N = \boldsymbol{R}'_T \cdot \boldsymbol{R}_Y \tag{6}$$

with

$$\boldsymbol{R}_N = (\boldsymbol{R}_{M1})^{-1}\boldsymbol{R}_{M2} = \begin{bmatrix} n_{11} & n_{12} \\ n_{21} & n_{22} \end{bmatrix} \tag{7}$$

and

$$\boldsymbol{R}'_T = (\boldsymbol{R}_{T1})^{-1} \cdot \boldsymbol{R}_{T2}. \tag{8}$$

In order for (6) to be mathematically identical to (have the same solution as) (3), it is rewritten as follows:

$$(\boldsymbol{R}_N)^T \cdot (\boldsymbol{R}_Y)^T = (\boldsymbol{R}_Y)^T \cdot (\boldsymbol{R}'_T)^T \tag{9}$$

where the superscript T indicates matrix transposition.

C. General Solution for the Transmission Problem

Equations (3) and (9) are the well-known similar equation relationships linking similar matrices $\boldsymbol{R}_M$ and $\boldsymbol{R}_T$, and $(\boldsymbol{R}_N)^T$ and $(\boldsymbol{R}'_T)^T$ respectively. We shall first solve for (3).

1) Solution for $\boldsymbol{R}_X$: Similar equations have the following properties:

- $\boldsymbol{R}_M$ and $\boldsymbol{R}_T$ have identical characteristic (eigen)values λ_1 and λ_2.
- These characteristic values may be written in matrix form (the spectral matrix):

$$\Lambda = \begin{bmatrix} \lambda_1 & 0 \\ 0 & \lambda_2 \end{bmatrix}.$$

- If the transforming matrices composed of the characteristic (eigen)vectors of $\boldsymbol{R}_M$ and $\boldsymbol{R}_T$ are designated, respectively, $\boldsymbol{M}$ and $\boldsymbol{T}$, we can write

$$\boldsymbol{R}_M = \boldsymbol{M} \cdot \Lambda \cdot \boldsymbol{M}^{-1} \tag{10}$$

$$\boldsymbol{R}_T = \boldsymbol{T} \cdot \Lambda \cdot \boldsymbol{T}^{-1}. \tag{11}$$

Consider the case where $\boldsymbol{R}_{T1}$ represents the through connection, i.e., $\boldsymbol{R}_{T1} = \boldsymbol{U}$, the unitary matrix, and $\boldsymbol{R}_{T2}$ is a matrix representing a reflectionless line of electrical length l between $\boldsymbol{X}$ and $\boldsymbol{Y}$. Thus

$$\boldsymbol{R}_{T2} = \begin{bmatrix} e^{-\gamma l} & 0 \\ 0 & e^{\gamma l} \end{bmatrix} \tag{12}$$

where γ is the complex propagation constant. Since

$$\boldsymbol{R}_T = \boldsymbol{R}'_T = \boldsymbol{R}_{T2}$$

$$= \boldsymbol{T} \cdot \Lambda \cdot \boldsymbol{T}^{-1} = \begin{bmatrix} e^{-\gamma l} & 0 \\ 0 & e^{\gamma l} \end{bmatrix} \tag{13}$$

we may conclude that the characteristic values of $\boldsymbol{R}_T$ and $\boldsymbol{R}_M$ are $\lambda_1 = e^{-\gamma l}$ and $\lambda_2 = e^{\gamma l}$. Substitution of (10) and (11) into (3) enables us to obtain, after some simple manipulation,

$$\boldsymbol{M} \cdot \Lambda \cdot \boldsymbol{M}^{-1} = \boldsymbol{R}_X \boldsymbol{T} \cdot \Lambda \cdot (\boldsymbol{R}_X \boldsymbol{T})^{-1}$$

from which we obtain

$$\boldsymbol{R}_X = \boldsymbol{M}\boldsymbol{T}^{-1} \triangleq \boldsymbol{M} \tag{14}$$

since the transforming matrix of $\boldsymbol{T}$ is the unitary matrix multiplied by constants set equal to unity in this case.

2) Solution for $\boldsymbol{R}_Y$: The quantities $(\boldsymbol{R}'_T)^T$ and $(\boldsymbol{R}_N)^T$ will have the same characteristic roots $\lambda_1 = e^{-\gamma l}$ and $\lambda_2 = e^{\gamma l}$ as in the previous case since $\boldsymbol{R}_T = (\boldsymbol{R}'_T)^T$. The coordinate transforming equation for $(\boldsymbol{R}_N)^T$ is

$$(\boldsymbol{R}_N)^T = \boldsymbol{N}^T \cdot \Lambda \cdot (\boldsymbol{N}^T)^{-1} \tag{15}$$

from which we may define, as with (14),

$$\boldsymbol{R}_Y^T \triangleq \boldsymbol{N}^T. \tag{16}$$

D. Particular Solutions

1) Characteristic Vectors for $\boldsymbol{R}_X$: The characteristic vectors of $\boldsymbol{R}_X$ may be written arbitrarily as

$$\boldsymbol{M} = \begin{bmatrix} k\bar{a} & p\bar{b} \\ k & p \end{bmatrix} \tag{17}$$

where k and p are unknown complex constants yielding the particular solution corresponding to the error matrix $\boldsymbol{X}$. The terms $\bar{a}$ and $\bar{b}$ are obtained by setting the second term of each characteristic vector equation to unity. The R parameters of error matrix $\boldsymbol{X}$ are, in terms of its S parameters,

$$\boldsymbol{M} = \frac{1}{(S_{12})_X} \begin{bmatrix} (S_{12})_X^2 - (S_{11})_X (S_{22})_X & (S_{11})_X \\ -(S_{22})_X & 1 \end{bmatrix}. \tag{18}$$

A term-by-term comparison between (17) and (18) reveals that two independent linear equations are necessary in order to solve for k and p. The fact that the error networks are reciprocal, being passive and nongyromagnetic, gives the *first* of these, and enables us to set the determinant of $\boldsymbol{M}$ to unity [9], [10]:

$$p \cdot k = \frac{1}{(\bar{a} - \bar{b})}. \tag{19}$$

A second passivity equation, the relationship $|S_{11}|^2 = |S_{22}|^2$, is difficult to exploit since it has several solutions.

A similar mathematical treatment may be applied to network $\boldsymbol{Y}$:

$$\boldsymbol{N}^T = \begin{bmatrix} r\bar{c} & s\bar{d} \\ r & s \end{bmatrix} \tag{20}$$

where r and s are the unknown complex constants corresponding to the particular solution required for error matrix $\boldsymbol{Y}$, and $\bar{c}$ and $\bar{d}$ are the vectors obtained by setting the second term of each characteristic vector equation to unity.

The reciprocity condition corresponding to (17) is, for network $\boldsymbol{Y}$,

$$r\cdot s=\frac{1}{(\bar{c}-\bar{d})}. \tag{21}$$

2) Coupled Matrices: The main problem with two-port lossless calibrations is that the input and output networks are inextricably linked, as can be seen by substituting the characteristic vector matrices $\boldsymbol{M}$ and $\boldsymbol{N}$ (eqs. (17) and (20)) into (1):

$$\boldsymbol{R}_{M1}=\begin{bmatrix} kr\cdot\bar{a}\bar{c}+ps\cdot\bar{b}\bar{d} & kr\cdot\bar{a}+ps\cdot\bar{b} \\ kr\cdot\bar{c}+ps\cdot\bar{d} & kr+ps \end{bmatrix}. \tag{22}$$

Each term in (22) is a function of constants kr and ps, and the input and output network matrices are thus coupled. One way of decoupling them is to use a very lossy two-port calibration network [12]; another is to disconnect $\boldsymbol{X}$ and $\boldsymbol{Y}$ and apply a reflective load to each. Before doing this, however, we observe that the ratio of the second term of (22) to the fourth gives the following useful relationship:

$$(S_{11})_{M1}=\frac{p^2\cdot(s/r)(\bar{a}-\bar{b})\bar{b}+\bar{a}}{p^2\cdot(s/r)(\bar{a}-\bar{b})+1} \tag{23}$$

or

$$ps=\pm\sqrt{\frac{((S_{11})_{M1}-\bar{a})}{(\bar{b}-(S_{11})_{M1})(\bar{a}-\bar{b})(\bar{c}-\bar{d})}}. \tag{24}$$

3) Symmetrical Error Network: If the error matrix $\boldsymbol{X}$ is *symmetrical* we can further apply the relationship $S_{11}=S_{22}$ in order to obtain a *second* linear relationship:

$$k=-p\bar{b}$$

whence

$$p=\pm\sqrt{\frac{1}{\bar{b}(\bar{b}-\bar{a})}}. \tag{25}$$

The sign of p depends on the physical length of the error network $\boldsymbol{X}$, since this affects the transmission phase $(S_{12})_X$, as shown by Meys [8]. Having solved for p, k is obtained from (19), and the error matrix $\boldsymbol{X}$ is fully resolved.

$\boldsymbol{Y}$ may be obtained by applying the same approach, in which case the relevant equations are

$$r=-s\bar{d}$$

and

$$s=\pm\sqrt{\frac{1}{\bar{d}(\bar{d}-\bar{c})}}. \tag{26}$$

Note that if *either* $\boldsymbol{R}_X$ *or* $\boldsymbol{R}_Y$ is obtained by applying this symmetry property, the unknown matrix ($\boldsymbol{R}_Y$ or $\boldsymbol{R}_X$) is obtained by inverse matrix multiplication from (1). This method, which may be termed the through-delay approach, has never, to the authors' knowledge, explicitly appeared in the literature, although similar methods are described in [7]–[9].

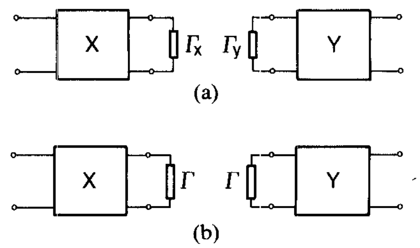

Fig. 3. (a) Reflect measurement using two known reflective loads Γ_Y and Γ_Y. (b) Reflect measurement using the same load Γ on the device connection port of both adapters.

4) $(S_{12})_X=(S_{12})_Y$*:* A special case of the through-delay approach has been brought to the author's attention [11] where $(S_{12})_X=(S_{12})_Y$. Application of this condition using (17), (20), and (22) yields

$$p=s \tag{27a}$$

$$\left(\frac{1}{kr+ps}\right)=(S_{21})_{M1} \tag{27b}$$

after which the parameters k and r are obtained from (19) and (21) respectively.

E. Reflective Measurement

There are two approaches described in the literature: two well-known reflective loads Γ_X and Γ_Y are applied independently to the "free" ports of the error networks $\boldsymbol{X}$ and $\boldsymbol{Y}$ [1], [2], and an unknown reflective load Γ is applied to each of the error networks $\boldsymbol{X}$ and $\boldsymbol{Y}$ in turn [3]–[6]. Consider each case in turn.

1) Known Reflective Loads Γ_X *and* Γ_Y*:* The approach followed is summarized in Fig. 3. The reflection coefficient Γ_1 is measured on the network analyzer with load Γ_X attached to error network $\boldsymbol{X}$, and Γ_2 is measured with Γ_Y connected to $\boldsymbol{Y}$. Consider the case of $\boldsymbol{X}$:

$$\Gamma_1=(S_{11})_X+\left[\frac{(S_{12})_X(S_{21})_X\Gamma_X}{1-(S_{22})_X\Gamma_X}\right] \tag{28}$$

or

$$\Gamma_1=\frac{p\bar{b}+k\bar{a}\cdot\Gamma_X}{p+k\cdot\Gamma_X}$$

whence

$$p=\pm\sqrt{\frac{\Gamma_X(\bar{a}-\Gamma_1)}{(\bar{a}-\bar{b})(\Gamma_1-\bar{b})}} \tag{29}$$

where (29) is obtained by applying (19). The error matrix $\boldsymbol{Y}$ may be resolved in an identical manner:

$$s=\pm\sqrt{\frac{\Gamma_Y(\Gamma_2+\bar{c})}{(\bar{c}-\bar{d})(\Gamma_2+\bar{d})}}. \tag{30}$$

2) Unknown Reflective Load Γ*:* This case is summarized schematically in Fig. 4. Since $\Gamma_X=\Gamma_Y=\Gamma$, multiplication

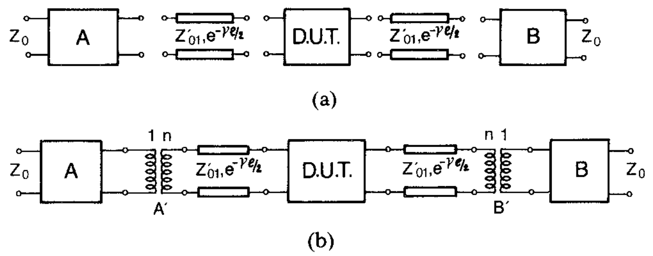

Fig. 4. (a) Two-port measurement problem applied to a device embedded in a non-50-Ω environment. (b) Introduction of two fictitious impedance transformers to convert between Z_0 and Z'_{01}.

of (29) and (30) yields

$$ps = \pm\sqrt{\frac{\Gamma^2(\bar{a}-\Gamma_1)(\Gamma_2+\bar{c})}{(\bar{a}-\bar{b})(\bar{c}-\bar{d})(\Gamma_1-\bar{b})(\Gamma_2+\bar{d})}}. \quad (31)$$

Equating (31) and (24) gives

$$\Gamma = \pm\sqrt{\frac{((S_{11})_{M1}-\bar{a})(\Gamma_1-\bar{b})(\Gamma_2+\bar{d})}{((S_{11})_{M1}-\bar{b})(\Gamma_1-\bar{a})(\Gamma_2+\bar{c})}}. \quad (32)$$

Equation (32) is identical to that derived in [3] in a rather more complicated manner. Having obtained Γ, the parameters p and s are calculated from (29) and (30), and k and r are obtained from (19) and (21) respectively.

III. Discussion

Although the mathematical approach we have outlined above is concise and readily programmable, it does give rise to several equations in which a sign ambiguity exists. We shall **now** consider the physical meaning of the parameters in order to arrive at the correct result.

The first of these ambiguities concerns the roots λ_1 and λ_2; it is simply resolved since the roots are reciprocal, and the root $\lambda_1 = \exp(-\gamma l)$ is that having a modulus less than unity:

$$\lambda_1 = e^{-\alpha}(\cos\beta + j\sin\beta) \quad (33)$$

where the propagation constant $\gamma = \alpha + j\beta$.

The second ambiguity concerns the characteristic vectors a and b for the input error network and c and d for the output error network. Although the vectors correspond, respectively, to roots λ_1 and λ_2, the relationship between these roots is such that an identical equation for vectors a and b is obtained [3], [4]:

$$\left.\begin{matrix}\bar{a}\\ \bar{b}\end{matrix}\right\} = -\frac{(m_{22}-m_{11})}{2m_{21}} \pm \sqrt{\left[\frac{m_{22}-m_{11}}{2m_{21}}\right]^2 + \frac{m_{12}}{m_{21}}} \quad (34)$$

where m_{11}, m_{12}, m_{21}, and m_{22} are defined (4). Since $|\bar{b}|$, the error linked to the reflection coefficient of the input reflectometer, will be much smaller than $|\bar{a}|$, the correct sign can be apportioned to each. In an identical manner, the vectors $\bar{c}$ and $\bar{d}$ are selected knowing that $|\bar{d}| \ll |\bar{c}|$ [3].

In the symmetrical matrix case (eqs. (25) and (26)) and the reflective load cases (eqs. (29) and (30)) further sign ambiguities occur, this time for the constants p and s. However, when using the error matrices $\boldsymbol{R}_X$ and $\boldsymbol{R}_Y$ for inverse matrix multiplication in order to correct unknown measured data, the constants k, p, r, and s do not appear alone but rather in pairs (ps, ks, pr, and kr), as can be seen from the following:

$$\boldsymbol{R}_{Tdut} = (\boldsymbol{R}_X)^{-1}\boldsymbol{R}_{Mdut}(\boldsymbol{R}_Y)^{-1}$$

or

$$\begin{bmatrix} t'_{11} & t'_{12} \\ t'_{21} & t'_{22}\end{bmatrix} = \begin{bmatrix} p & -p\bar{b} \\ -k & k\bar{a}\end{bmatrix}\cdot\begin{bmatrix} m'_{11} & m'_{12} \\ m'_{21} & m'_{22}\end{bmatrix}\cdot\begin{bmatrix} s & -r \\ -s\bar{d} & r\bar{c}\end{bmatrix} \quad (35)$$

$$\begin{bmatrix} t'_{11} & t'_{12} \\ t'_{21} & t'_{22}\end{bmatrix} = \begin{bmatrix} psT'_1 & -prT'_2 \\ -ksT'_3 & krT'_4\end{bmatrix} \quad (36)$$

where $\boldsymbol{R}_{Mdut}$ (elements $m'_{11}, m'_{12}, m'_{21}, m'_{22}$) represents the cascade matrix form of the measured S parameters corresponding to device-under-test $\boldsymbol{R}_{Tdut}$ (elements $t'_{11}, t'_{12}, t'_{21}, t'_{22}$), and T'_1, T'_2, T'_3, and T'_4 are functions of the previously calculated vectors $\bar{a}, \bar{b}, \bar{c}, \bar{d}$ and $m'_{11}, m'_{12}, m'_{21}, m'_{22}$.

The sign ambiguity is lifted for ps and kr by applying successively different signs to them and substituting these values and those of $\bar{a}$, $\bar{b}$, $\bar{c}$, and $\bar{d}$ into (36) for the case of the delay line. We thereby obtain the signs of ps and kr in terms of $e^{-\gamma l}$ and $e^{\gamma l}$, known quantities which have been derived independently:

$$ps = e^{-\gamma l}/T'_1 \quad (37a)$$

$$kr = e^{\gamma l}/T'_4. \quad (37b)$$

Multiplication of (19) and 37(a) and of (19) and (37b) enables us to determine the signs of ks and pr respectively.

Finally, in the self-calibration case (eq. (32)), the sign of Γ is obtained from an approximate knowledge of its phase (short circuit or open circuit) [3], [4].

IV. Applications

A. Arbitrary Line Impedance Standards

Although non-50-Ω standards have been used in an *ad hoc* manner for many years, particularly for on-wafer measurements, no theoretical justification has appeared in the technical literature. Such a justification is, however, easy to obtain by applying the mathematical approach.

Consider the case, typical in GaAs on-wafer measurements, where a non-50-Ω line of impedance Z'_{01} is fed via two error matrices $\boldsymbol{A}$ and $\boldsymbol{B}$ from a 50 Ω environment (Fig. 4(a)). In order to understand how the through-delay reflect approach automatically corrects for the change in line impedance *provided that the standards are realized with the same line impedance*, consider the use of two hypothetical impedance transformers, $\boldsymbol{A}'$ and $\boldsymbol{B}'$, applied respectively to ports A and B (Fig. 4(b)). Note that, as in the case of Meys [8], the two transformers $\boldsymbol{A}'$ and $\boldsymbol{B}'$ are identical, but with input and output ports inverted. Fig. 5 illustrates schematically how the correction for $\boldsymbol{A}'$ and $\boldsymbol{B}'$ may be made by integrating the transformers into the error

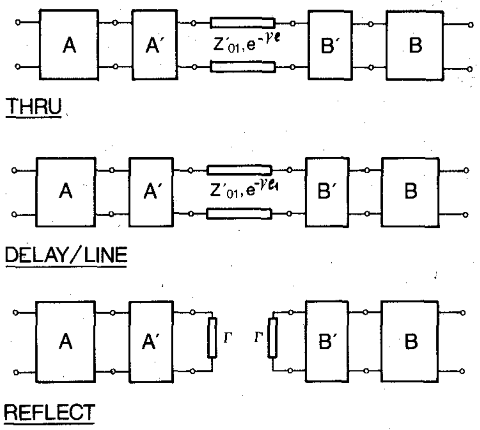

Fig. 5. Application of the through-delay-reflect technique to correct for error adapters including impedance transformers A' and B'.

networks, (1) and (2) thereby becoming

$$R_{M1} = (R_A R_{A'}) \cdot R_{T1} \cdot (R_{B'} R_B) \tag{37}$$

$$R_{M2} = (R_A R_{A'}) \cdot R_{T2} \cdot (R_{B'} R_B) \tag{38}$$

and the methods outlined in Section II now apply (Fig. 5) with R_{Tdut}, the unknown device parameters, normalized to Z'_{01}.

B. Other Calibration Standards

The mathematical approach described may also be used to analyze the different calibration standards described in [12], with the proviso that these must include *two known two-port calibration networks* (i.e., (1) and (2) must exist). In the example of the through-attenuation network cited in [12], if the through standard is used to obtain (1) and the known two-port network is used to obtain (2), the final attenuation calibration network need only be reciprocal for the error networks R_X and R_Y to be solved. The derivation of the relevant equations pertaining to this case is too long to include in this paper, and will form the basis of another article.

V. Conclusion

A unified mathematical treatment of the various approaches to the through-delay-reflect calibration problem has been presented. The prime advantage of a rigorous description of the two-port error-correction problem is that it enables the *mathematical validity* of the various calibration techniques to be easily appreciated and innovative calibration methods to be derived.

Acknowledgment

The authors are indebted to S. Meszaros of the Communications Research Centre (Ottawa) for her help in checking each of the cases treated in this paper. They would also like to thank the directors of the Centre National d'Etudes des Telecommunications for their permission to publish this article.

References

[1] N. R. Franzen and R. A. Speciale, "A new procedure for system calibration and error removal in automated S-parameter measurements," in *Proc. 5th European Microwave Conf.*, Sept. 1975, pp. 69–73.

[2] R. A. Speciale, "A generalization of the TSD network analyzer calibration procedure, covering n-port scattering parameter measurements, affected by leakage errors," *IEEE Trans. Microwave Theory Tech.*, vol. MTT-25, pp. 1100–1115, Dec. 1977.

[3] D. Rytting, "An analysis of vector measurement accuracy techniques," in *Proc. Hewlett-Packard RF and Microwave Symp.*, 1980 (see appendix).

[4] M. Parisot and R. A. Soares, *GaAs MESFET Circuit Design*, R. Soares, Ed. Norwood, MA: Artech House, 1988, ch. 3.

[5] G. F. Engen and C. A. Hoer, "Thru-reflect-line: An improved technique for calibrating the dual six-port automatic network analyzer," *IEEE Trans. Microwave Theory Tech.*, vol. MTT-27, pp. 987–998, Dec. 1979.

[6] C. A. Hoer and G. F. Engen, "Calibrating a dual six-port or four-port for measuring two-ports with any connector," in *IEEE MTT-S Int. Microwave Symp. Dig.* (Baltimore), 1986, pp. 665–668.

[7] E. R. Ehlers, "Symmetric test fixture calibration," in *IEEE MTT-S Int. Microwave Symp. Dig.* (Baltimore) 1986, pp. 275–278.

[8] R. P. Meys, "A triple-through method for characterizing test fixtures," *IEEE Trans. Microwave Theory Tech.*, vol. 36, pp. 1043–1046, June 1988.

[9] R. Soares, P. Gouzien, and P. Legaud, "Matching network characterization by S-parameter measurements of two-port active devices," *Proc. Inst. Elec. Eng.*, vol. 135, pp. 426–430, Dec. 1988.

[10] K. C. Gupta, R. Garg, and R. Chadha, *Computer-Aided Design of Microwave Circuits*. Norwood, MA: Artech House, 1981, pp. 319–321.

[11] AVANTEK Application Note: "Measurement and modelling of GaAs FET chips," Avantek, Inc., Santa Clara, CA, Oct. 1983.

[12] H-J. Eul and B. Schiek, "Thru-match-reflect: One result of a rigorous theory for de-embedding and network analyzer calibration," in *Proc. 18th European Microwave Conf.*, Sept. 1988, pp. 909–914.

Robert A. Soares (M'87) was born in Bombay, India, and was educated at St. Joseph's College, Darjeeling. He received the B.Sc. (Hons, 1967) and Ph.D. (1975) degrees in electronic engineering from the University of London, United Kingdom.

He started working in the microwave field at the GEC Hirst Research Centre, U.K. (1970–1973) on S-band low-noise bipolar amplifier design. In 1974, he joined the Plessey Allen Clark Research Centre, Caswell, U.K., where he worked on X-band low-noise GaAs MESFET characterization and amplifier design. He has been at the Centre National d'Etudes des Telecommunications (CNET), Lannion, France, since November 1976, where he has successively worked on power GaAs MESFET characterization and amplifier design, nonlinear modeling, dielectric resonator oscillators, and frequency multipliers. Since 1983 he has worked on GaAs MESFET amplifier design at 20 and 30 GHz, and is currently project leader on a MHMIC (miniaturized hybrid microwave integrated circuit) development effort at CNET.

Dr. Soares is a member of the IEE, has authored or coauthored over 30 technical articles, and holds one patent. He is the main author and editor of *GaAs MESFET Circuit Design* (1988, Artech House) and coeditor of *Applications of GaAs MESFETs* (1983, Artech House) and *Applications des Transistors à Effet de Champ en Arseniure de Gallium* (1984, Eyrolles).

Pascal Gouzien was born in St. Renan, Finistere, France, on October 10, 1953. He received the "Licences es Telecommunications" degree from the University of Limoges.

He is currently engaged in microwave circuit computer-aided layout and computer-aided measurement studies at the Centre National d'Etudes des Telecommunications (CNET), Lannion, France.

Pierre Legaud was born in Lannion, France, on August 4, 1953. He received the "Diplome Universitaire de Technologie" from the University Institute of Technology, Lannion.

He started working in the field of microwaves at THOMSON CSF Avionics at Malakoff, Paris, in 1974. He joined the Centre National d'Etudes des Telecommunications (CNET), Lannion, in 1983, where he is now working on GaAs MESFET low-noise amplifier design at 20 and 30 GHz.

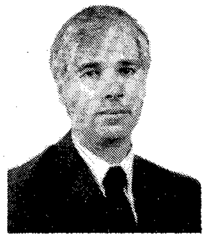

Georges Follot was born in Beaune, France, on October 20, 1948. He was educated at Diderot High School in Laneres.

He began working with the French P.T.T. in 1971. He has been involved in microwaves since 1988 at the Centre National d'Etudes des Telecommunications (CNET), Lannion, France.